Research Square

Preprints are preliminary reports that have not undergone peer review.
They should not be considered conclusive, used to inform clinical practice,
or referenced by the media as validated information.

Gaussian Process–Based Bayesian Optimization of Lower-Limb PNS–TMS Interstimulus Intervals in Adults and Children: A Proof-of-Concept Toward a Personalized Framework

Mohammad Reza Effatparvar
Université de Montréal
Mathilde Tardif
Université de Montréal
Mauricio Rivera
Université de Montréal
Mickaël Begon
Université de Montréal
Marco Bonizzato
Polytechnique Montréal
Yosra Cherni
yosra.cherni@umontreal.ca

Université de Montréal

Research Article

Keywords: transcranial magnetic stimulation, peripheral nerve stimulation, motor evoked potential, interstimulus interval, Gaussian process regression, Bayesian optimization, neuromodulation

Posted Date: September 8th, 2026

DOI: https://doi.org/10.21203/rs.3.rs-10841219/v1

License: This work is licensed under a Creative Commons Attribution 4.0 International License. Read Full License

Additional Declarations: No competing interests reported.

Abstract

Background

Peripheral nerve stimulation (PNS) before transcranial magnetic stimulation (TMS) can modulate lower-limb motor evoked potentials (MEPs), but individualized interstimulus interval (ISI) selection remains unclear, particularly in children.

Methods

Ten adults and eight children were tested. Common peroneal nerve PNS preceded TMS of the tibialis anterior (TA) hotspot at 26 latency-referenced ISIs. Adults completed sensory- and motor-threshold PNS; children completed motor-threshold PNS only. Gaussian process (GP) regression modeled ISI–response profiles, and retrospective GP-based Bayesian optimization (GPBO) was benchmarked against random sampling, with population-informed initialization evaluated separately.

Results

In adults, PNS condition, ISI, and their interaction significantly affected TA, soleus, and gastrocnemius responses (all $p < 0.001$); in children, ISI significantly affected all three muscles. GP regression reproduced motor-threshold TA profiles with mean R^2 values of 0.91 in adults and 0.66 in children, with leave-one-ISI-out R^2 values of 0.71 and 0.18. GP regression improved profile recovery with one repetition per ISI. In adults, GPBO reached threshold in 9/10 participants with a median of 10 [IQR: 8–17] stimulations versus 20 [13–66] with random sampling (9/10). In children, corresponding values were 45 [24–60] in 5/8 versus 56 [35–79] in 4/8. Population-informed initialization provided no consistent benefit.

Conclusion

Lower-limb PNS–TMS responses are timing dependent and individualized. GP modeling and GPBO may support efficient individualized ISI characterization, particularly in adults. Greater pediatric response variability and weaker predictability may make reliable identification of a consistently high-performing ISI more difficult.

1. Introduction

Understanding how sensory input from the lower limb interacts with corticospinal excitability is important for developing neuromodulation protocols targeting motor function. One way to assess this interaction is to deliver peripheral nerve stimulation (PNS) before transcranial magnetic stimulation (TMS) and measure the resulting motor evoked potential (MEP) [1]. This conditioned response depends on several interrelated parameters, including the stimulated nerve, target muscle, stimulation site, stimulation intensity, muscle activation state, as well as interstimulus interval (ISI) [2]. Among these parameters, ISI is particularly important because it determines the timing between the afferent volley and the TMS-evoked corticospinal response. Changes in ISI can therefore substantially alter the magnitude of the conditioned MEP and may shift the response direction between facilitation and inhibition [3].

In upper-limb studies, paired PNS-TMS protocols have been widely used to probe sensorimotor integration and corticospinal excitability, with specific ISI ranges associated with short-latency afferent inhibition, long-latency afferent inhibition, and afferent-induced facilitation [4, 5]. In the lower limb, available evidence also shows that peripheral afferent input can condition TMS-evoked responses in leg muscles [6–8]. Therefore, systematic mapping of lower-limb conditioned MEP responses across a broad, dense range of timing intervals, stimulation intensities, and muscles may

help explore lower-limb ISI–response profiles and evaluate whether model-based approaches can efficiently identify individualized facilitatory ISIs.

This approach may be particularly useful because the ISI producing the strongest acute facilitation is unlikely to be uniform across participants, muscles, or stimulation conditions. At the group level, dense ISI sampling can help determine whether consistent response patterns are present across muscles, PNS intensities, and age groups. At the individual level, modeling the ISI–response relationship may help estimate participant-specific facilitatory timings that would be difficult to define using only a small number of predefined ISIs. Gaussian process regression is well suited to this objective because it can model potentially non-linear and noisy ISI–response relationships while quantifying uncertainty across the response profile [9]. When combined with Bayesian optimization (BO), this uncertainty can guide sampling toward candidate facilitatory ISIs and evaluate whether individualized timings can be identified with fewer stimulations than exhaustive testing [10].

Within this data-driven framework, the present study used dense grid-search sampling of latency-referenced ISIs to examine lower-limb conditioned MEP responses across PNS intensities in healthy adults and children. The objectives were: (1) to explore participant-specific ISI–response profiles across stimulation conditions; (2) to evaluate whether Gaussian process regression could model these profiles using fewer repetitions; and (3) to assess whether GP-based BO could efficiently identify individualized high-performing ISIs, including through population-informed initialization.

2. Methods

2.1 Participants

Eighteen healthy volunteers were recruited for this study, including ten adults (18 to 35 years) and eight children (7 to 13 years). The adult group comprised six females (26.0 ± 4.9 years) and four males (27.5 ± 4.5 years), and the children group comprised five females (10.0 ± 2.4 years) and three males (9.3 ± 1.5 years). Participants were eligible if they were in stable health and had no known neurological, musculoskeletal, or orthopedic condition that could affect lower-limb function or voluntary ankle movement, and no contraindications to TMS or PNS [11–12].

The study was approved by the Research Ethics Committee of Université de Montréal (protocol no. 2026–9243; approved 19 February 2026) and was conducted in accordance with the Declaration of Helsinki. All adult participants provided written informed consent prior to participation. For children, written informed consent was obtained from a parent or legal guardian, and verbal or written assent was obtained from the child when appropriate.

2.2 Experimental setup

Participants were seated comfortably in a chair with the hip and knee flexed at approximately 90°. The right foot was placed on a step positioned in front of the chair. Wireless surface electromyography (EMG) sensors (Delsys Trigno, Delsys Inc., Boston, MA, USA) were placed over the tibialis anterior (TA), soleus (SOL), and gastrocnemius medialis (GAS) of the right leg following skin preparation and standard anatomical placement procedures [13]. EMG signals were acquired using the manufacturer's default hardware configuration in Trigno Utility software with a sampling rate of 4352 Hz, an input range of 22 mV, and a 10–450 Hz hardware band-pass filter. To standardize the active ankle position used during stimulation, 10° of ankle dorsiflexion was first measured for each participant. An adjustable mechanical stop attached to the step was then positioned to prevent movement beyond this angle.

EMG signals and stimulation trigger channels were acquired using a CED Micro1401 data acquisition interface (Cambridge Electronic Design, Cambridge, UK) and recorded using Signal software (CED, Cambridge, UK), allowing synchronized recording of EMG activity, TMS triggers, and PNS triggers throughout the protocol.

2.3 Transcranial magnetic stimulation protocol

TMS was delivered over the motor cortex contralateral to the right leg using a Magstim Rapid2 stimulator (Magstim, Dyfed, UK) connected to a figure-of-eight coil. Coil position was identified and monitored in real time using a Brainsight neuronavigation system (Rogue Research, Montreal, Canada). The stimulation hotspot for the TA was identified as the scalp position that consistently produced the largest MEPs in the TA. Resting motor threshold (RMT) was defined as the lowest stimulation intensity able to evoke a discernible MEP in at least 5 of 10 trials while the foot was at rest. Active motor threshold (AMT) was defined as the lowest stimulation intensity able to evoke a discernible MEP in at least 5 of 10 trials during an active ankle dorsiflexion. After identifying the hotspot, 10 unconditioned single-pulse TMS stimuli were delivered during active ankle dorsiflexion at 120% RMT when RMT could be identified, or at 120% AMT otherwise [14–15]. These responses were used to determine baseline corticospinal excitability and MEP latency. The same TMS intensity was used during the PNS-TMS protocol in order to elicit stable conditioned responses of sufficient amplitude [16].

2.4 Peripheral nerve stimulation protocol

PNS was delivered to the common peroneal nerve (CPN) of the right leg using a RehaStim P24 electrical stimulator (HASOMED GmbH, Magdeburg, Germany). Stimulation was applied through surface electrodes positioned over the fibular head region to target the CPN. Stimulation consisted of biphasic pulses with a pulse width of 1 ms. For each participant, two PNS thresholds were determined. Sensory threshold was defined as the lowest intensity at which the participant consistently perceived the pulse [17]. Motor threshold was defined as the lowest intensity that produced a visible ankle dorsiflexion. In adults, both sensory- and motor-threshold PNS conditions were applied but in children, only the motor-threshold PNS condition was applied to minimize the burden and ensure feasibility. The complete experimental setup, including participant positioning, EMG recording, TMS, and PNS components, is shown in Fig. 1.

2.5 PNS-TMS protocol

The paired stimulation was performed using a conventional paired-pulse paradigm in which one PNS pulse was paired with one TMS pulse at a frequency of 0.1 Hz, corresponding to one stimulus pair every 10 s [18]. During the stimulations, the PNS pulse served as the trigger event, and the TMS pulse was delivered after a predefined ISI controlled in Signal software.

For each participant, the ISI search space was individualized and ranged from MEP latency + 5 ms to MEP latency + 130 ms, in increments of 5 ms, resulting in 26 ISIs. This generated a broad latency-referenced ISI space intended to capture facilitatory, inhibitory, and intermediate conditioned responses [18–19]. The order of tested ISIs was randomized for each participant.

In adults, all 26 ISIs were tested under both sensory- and motor-level PNS conditions, with 10 repetitions per ISI × PNS combination, resulting in 520 paired stimulations per participant. In children, only motor-level PNS was tested, with 6 repetitions at each of the 26 ISIs, resulting in 156 paired stimulations per participant.

To ensure consistent muscle activation and reduce sustained effort during repeated stimulation, participants performed brief active dorsiflexion only when instructed. A standardized auditory cue generated by the acquisition system indicated alternating active and rest periods for each repetition.

A schematic overview of the full study procedure, including paired-stimulation timing, individualized ISI mapping, repetition structure, and downstream analysis, is shown in Fig. 2.

2.6 Pain, fatigue, and maximal voluntary contractions

To assess protocol tolerability, participants rated perceived pain using a Numeric Rating Scale (0–10) [20] and perceived fatigue using the Borg CR10 scale (0–10) [21]. Ratings were obtained after completion of each PNS-TMS set (10

repetitions in adults and 6 repetitions in children) to assess whether ratings varied as a function of stimulation intensity, ISI, or test order. To further examine possible fatigue-related effects of the protocol, maximal voluntary contractions (MVCs) were recorded before and after PNS-TMS testing. Three MVC trials were obtained for TA during resisted dorsiflexion, and three MVC trials were obtained for SOL and GAS during maximal plantarflexion. For pre–post session analyses, EMG amplitude was quantified using the root mean square (RMS) over the highest stable 3-s MVC window within each trial and averaged across the three trials obtained for each muscle.

2.7 Data Processing

EMG data were processed using MATLAB (R2022b). All EMG traces were visually inspected prior to analysis, and trials with major technical artifacts, absent or uninterpretable responses, or excessive contamination preventing reliable quantification were excluded. Because MEP waveform profiles were variable, with several responses showing multiphasic morphologies, area under the curve (AUC) was used instead of peak-to-peak amplitude to quantify the response.

For each participant and muscle, the AUC window started at the corresponding MEP latency. The end of the window was determined manually by visual inspection as the time point at which the MEP returned to baseline. Once selected, this window was kept fixed across all ISIs for that participant and muscle. The window was re-evaluated separately for each participant and muscle to account for individual differences in MEP timing and duration. Unconditioned TMS responses collected at baseline were processed using the same participant- and muscle-specific window to provide the individualized reference value. Window selection was performed by visual inspection and was not blinded to ISI.

For each participant and muscle, the mean AUC of the unconditioned TMS trials was used as the baseline reference. Each conditioned trial was normalized separately and expressed as the natural logarithm of the ratio between its conditioned AUC and the mean unconditioned AUC. This procedure yielded a trial-level baseline-referenced response for each participant, muscle, PNS condition, ISI, and repetition.

For analyses based on ISI-level response profiles, trial-level log-ratio responses were averaged across repetitions within each participant, muscle, PNS condition, and ISI. Individual trial-level responses were retained for the GP model-checking, data-efficiency, and retrospective Bayesian-optimization analyses. The mean response obtained from all available repetitions at each ISI was used as the reference ISI–response profile.

Positive and negative values indicated responses above and below the unconditioned baseline, respectively. Participant-specific response profiles were defined by the pattern of these responses across tested ISIs and stimulation conditions. These profiles were used to explore within-participant variation in conditioned responses across the individualized ISI search space.

2.8 Gaussian process regression

To model the relationship between conditioned response and stimulation timing, GP regression [9] was applied to the baseline-referenced response values described above. For each participant and stimulation condition, responses were averaged across repetitions at each ISI value, and a GP was fitted to the resulting participant-specific mean ISI responses. In addition, participant-specific mean responses were pooled within each age group, muscle, and PNS condition, and a separate GP was fitted to estimate the corresponding population-level ISI–response relationship.

Models were implemented in MATLAB using the GPML toolbox (https://gaussianprocess.org/gpml/) with a Matérn 5/2 kernel covariance function and Gaussian likelihood function. The kernel hyperparameters, including the length scale, signal variance, and observation-noise variance, were estimated using maximum a posteriori estimation with smooth-box priors. The nominal prior ranges were 5–60 ms for the length scale, 0.05–20 for the signal standard deviation, and 0.01–1.5 for the noise standard deviation. Participant-specific GP posterior means and approximate 95% credible intervals for

the latent ISI–response function were computed across the observed ISI range. The posterior mean was also computed for each pooled GP.

2.9 GP model evaluation

Because TA was the primary TMS target muscle and motor-threshold PNS was tested in both age groups, the principal GP model-evaluation, data-efficiency, and Bayesian-optimization analyses focused on motor-threshold TA responses in adults and children. Corresponding analyses for the other muscles and PNS conditions were considered secondary and are presented in the Supplementary Material.

GP performance was evaluated using the individual trial-level log-ratio responses. Models were assessed across predefined length scales ranging from 2.5 to 130 ms, with the signal and noise hyperparameters re-estimated at each length scale.

A participant-specific data-driven length scale was additionally estimated from the complete trial-level dataset using maximum a posteriori estimation with a wider nominal length-scale range of 1–300 ms. Model fit at the data-driven length scale was quantified using R^2 relative to both the individual trial responses and the complete per-ISI mean profile. The variance explained by the empirical per-ISI means was also calculated as an empirical reference ceiling for trial-level prediction.

Generalization to unobserved stimulation timings was assessed using leave-one-ISI-out cross-validation. In each fold, all trials from one ISI were excluded, and its mean response was predicted using a GP fitted to the remaining ISIs. Prediction performance was summarized using R^2 between the predicted and observed per-ISI mean responses. For each participant, leave-one-ISI-out performance was summarized at the predefined length scale that produced the highest cross-validation R^2.

2.10 Data-efficiency analysis

To examine whether GP modeling could estimate participant-specific response profiles using fewer repetitions, one to five trials were randomly selected without replacement at each ISI, subject to the number of available repetitions. Using the same selected trials, response profiles were estimated using either the empirical per-ISI mean or GP regression. Both profiles were compared with the reference profile obtained from all available repetitions using root mean square error (RMSE) and R^2. This procedure was repeated 200 times for each participant and number of repetitions.

2.11 Gaussian-process-based Bayesian optimization

A retrospective GPBO [10] replay analysis was performed to evaluate how efficiently participant-specific high-performing ISIs could be identified from sequential single-trial observations. For each participant, the mean response across all available repetitions at each ISI defined the reference response profile, and the ISI with the highest mean response was considered the reference optimum.

Each replay included up to 260 stimulation queries in adults and 156 stimulation queries in children, corresponding to the number of stimulations used in the complete motor-threshold mapping protocol. Each replay began with three randomly selected queries. Repeated selection of the same ISI was permitted during both the initial and subsequent queries.

At each query, one trial response was sampled with replacement from the available experimental responses at the selected ISI, such that each query represented one simulated paired stimulation. A GP model using the same kernel covariance function, likelihood function, and hyperparameter priors described above was updated after each observation.

From the fourth query onward, the next ISI was selected using GPBO, with Thompson sampling as the acquisition function. A value was independently sampled from the GP marginal posterior distribution at each candidate ISI, and the

ISI with the highest sampled value was selected. After each query, the current recommendation was defined as the previously sampled ISI with the highest GP posterior mean.

GPBO was compared with random ISI sampling. In the random condition, the next ISI was selected randomly, while the same GP model and recommendation rule were applied to the accumulated observations. Thus, the comparison evaluated the effect of the strategy used to select the next ISI. Each procedure was repeated 50 times per participant using different randomized query and trial-response sequences.

Optimization performance was primarily quantified using the normalized exploration score:

$$f_q = [f(\hat{x}_q) - f_{min}] / [f_{max} - f_{min}]$$

Where $f(\hat{x}_q)$ was the reference mean response at the currently recommended ISI, and f_{min} and f_{max} were the lowest and highest responses in the participant-specific reference profile. A score of 0 represented the lowest reference response, whereas a score of 1 represented the reference optimum. For each participant, exploration scores were averaged across the 50 replay runs at each stimulation query. The number of stimulations required for this participant-specific mean exploration-score curve to reach 0.90 was then recorded. Participants whose mean exploration-score curve did not reach 0.90 within the corresponding stimulation budget were classified as not reaching the threshold. For group-level visualization, the participant-specific mean exploration-score trajectories were averaged across participants and are presented as the group mean ± standard error of the mean.

2.12 Population-informed initialization

An exploratory analysis evaluated whether a population-informed prior could improve early optimization performance. For each participant, a population-level ISI–response profile was derived by interpolating the response profiles of all other participants onto the ISI grid of the participant being optimized and then averaging these profiles. The participant being optimized was excluded from this calculation, ensuring that their own data did not contribute to the prior. This population profile was used as the initial GP mean. Its influence was reduced exponentially with a time constant of five queries as participant-specific observations accumulated, allowing the model to increasingly reflect the individual response profile. Optimization using the population-informed prior was compared with GPBO using a zero-mean GP.

2.13 Statistical analysis

Descriptive statistics were computed for baseline measurements and expressed as mean ± SD. For the first objective of the study, MEP results were analyzed separately for each muscle using linear mixed-effects models, applied to the participant-level mean baseline-referenced responses at each ISI and PNS condition, with participant as a random intercept.

In adults, MEP results were modeled as a function of PNS condition, ISI, and their interaction, whereas in children, they were modeled as a function of ISI only. ISI was treated as a categorical factor. In adults, ISI effects were additionally examined separately within the motor- and sensory-threshold PNS conditions. Statistical significance was set at $p < 0.05$.

GP model-performance metrics were calculated separately for each participant and summarized across participants as mean ± SD. For the data-efficiency analysis, RMSE and R2 were first averaged across the 200 resampling iterations within each participant and then summarized across participants as mean ± SD. For Bayesian optimization, exploration-score curves were averaged across the replay runs within each participant. The stimulation count to threshold was defined as the first query at which the participant-specific mean exploration-score curve reached 0.90. The number of participants reaching the threshold was reported for each condition. Among participants reaching the threshold, stimulation counts were summarized as median [interquartile range (IQR)] because of their skewed distribution. Final exploration scores were summarized across all participants as mean ± standard error of the mean. For group-level visualization, participant-

specific mean exploration-score trajectories were averaged across participants and displayed as the group mean with the standard error of the mean.

For protocol tolerability, differences in pain and fatigue ratings between stimulation conditions were tested using paired Wilcoxon signed-rank tests, and associations with ISI and test order were assessed using Spearman rank correlations. Pre- to post-test changes in MVC were calculated for each participant and tested against zero using paired Wilcoxon signed-rank tests. All statistical analyses were performed in MATLAB (R2022b).

2.14 Use of generative AI and AI-assisted technologies

During preparation of this manuscript, one author (MRE) used ChatGPT (OpenAI) to support language editing and to assist in preparing Fig. 2. All AI-assisted content was reviewed, edited, and verified by the authors, who take full responsibility for the final content of the manuscript.

3. Results

3.1 Participant characteristics

All participants except one child completed the full experimental protocol. This child discontinued the session because of impatience, for reasons unrelated to the stimulation protocol. No adverse events were reported during or after testing. Baseline stimulation and electrophysiological characteristics are summarized in Table 1, with participant-specific conditioned responses presented in the Supplementary Material (Supplementary Figures S1–S6). Mean TA MEP latency was 30.29 ± 1.06 ms in adults and 24.58 ± 0.98 ms in children. In adults, the mean sensory-threshold and motor-threshold PNS amplitudes were 5.60 ± 1.64 mA and 21.40 ± 7.38 mA, respectively. In children, only motor-threshold PNS was tested, with a mean amplitude of 24.37 ± 6.18 mA. In adults, the mean RMT and AMT were 87.14 ± 11.65% MSO and 78.90 ± 11.50% MSO, respectively. In children, RMT could not be identified in the majority of participants; therefore, only AMT values are reported, with a mean AMT of 85.12 ± 7.60% MSO.

Table 1. Participant characteristics and baseline electrophysiological and stimulation parameters

Participant	Sex	Age	TA MEP latency, ms	RMT (%MSO)	AMT (%MSO)	Sensory PNS amplitude, mA	Motor PNS amplitude, mA	TA MEP AUC at 120% RMT/AMT, μV·ms	TA Background RMS, conditioned trials (μV)
Adult_01	M	25	30.47 ± 1.85	74	69	5	15	3742.17 ± 857.41	28.32 ± 2.58
Adult_02	F	24	28.61 ± 1.73	86	74	8	20	2409.88 ± 357.03	18.49 ± 2.50
Adult_03	M	24	30.91 ± 0.47	—	80	6	15	5915.09 ± 1754.13	51.12 ± 2.84
Adult_04	F	34	29.67 ± 1.21	90	77	7	15	3551.62 ± 580.97	21.63 ± 3.68
Adult_05	M	34	31.01 ± 1.55	70	59	4	16	5335.80 ± 943.69	21.92 ± 2.65
Adult_06	F	22	29.19 ± 1.21	100	74	3	30	7985.43 ± 1482.59	44.40 ± 4.00
Adult_07	M	27	32.44 ± 1.87	—	100	5	15	1732.76 ± 355.14	28.48 ± 2.09
Adult_08	F	24	29.26 ± 1.10	90	80	5	30	1775.03 ± 215.88	13.13 ± 2.49
Adult_09	F	30	30.76 ± 1.05	100	84	8	33	2085.37 ± 508.37	15.91 ± 1.77
Adult_10	F	22	30.66 ± 0.83	—	92	5	25	1951.72 ± 473.52	21.65 ± 2.79
Mean	**—**	**26.6 ± 4.5**	**30.29 ± 1.06**	**87.14 ± 11.65**	**78.9 ± 11.5**	**5.6 ± 1.64**	**21.4 ± 7.38**	**3648.48 ± 2021.09**	**25.54 ± 12.09**
Child_01	F	8	25.24 ± 0.91	—	88	3	28	1255.30 ± 500.11	21.69 ± 4.70
Child_02	M	11	25.29 ± 1.05	95	85	5	23	693.20 ± 205.64	19.58 ± 9.24
Child_03	M	9	24.22 ± 1.97	—	80	6	15	1834.62 ± 815.07	22.40 ± 3.83
Child_04	F	13	25.76 ± 1.22	—	78	3	20	2808.82 ± 1190.56	32.63 ± 3.50
Child_05	F	11	24.96 ± 1.21	—	74	6	27	2956.61 ± 840.99	26.26 ± 5.59
Child_06	F	7	23.29 ± 2.03	—	95	5	27	662.75 ± 439.39	17.41 ± 8.34
Child_07	F	11	23.03 ± 1.69	—	86	7	20	5806.02 ± 1581.83	57.21 ± 12.99
Child_08	M	8	24.85 ± 0.62	—	95	10	35	958.70 ± 509.91	37.83 ± 9.02

Table 1. Participant characteristics and baseline electrophysiological and stimulation parameters									
Mean	**—**	**9.7 ± 2.0**	**24.58 ± 0.98**	**—**	**85.12 ± 7.60**	**5.62 ± 2.26**	**24.37 ± 6.18**	**2122.00 ± 1736.09**	**29.38 ± 13.17**

3.2 Effects of ISI and PNS

Conditioned responses varied significantly with ISI and PNS condition. In adults, TA, SOL, and GAS all showed significant effects of PNS condition, ISI, and PNS × ISI interaction (all $p < 0.001$). When analyzed separately by PNS condition, ISI had a significant effect in the motor-threshold condition for all three muscles (all $p < 0.001$), but not in the sensory-threshold (TA: $p = 0.196$; SOL: $p = 0.108$; GAS: $p = 0.488$). In children, only motor-threshold PNS was tested, and ISI significantly affected TA ($p = 0.004$), SOL ($p < 0.001$), and GAS ($p < 0.001$).

3.3 Gaussian-process ISI–response profiles

GP profiles showed substantial variability in the magnitude, shape, and timing of conditioned responses across participants, muscles, and stimulation conditions (Fig. 3). In adults, the pooled motor-threshold profiles were predominantly below baseline at earlier ISIs and generally increased at later ISIs. For TA, the pooled response gradually increased from negative values at early ISIs to above-baseline values after approximately MEP + 95 ms. SOL showed a similar but more modest late increase, whereas GAS exhibited a less uniform profile, with small above-baseline responses at approximately MEP + 25–35 ms and again near MEP + 105–120 ms. In contrast, pooled sensory-threshold responses remained close to baseline across the tested ISIs for all three muscles.

In children, the pooled motor-threshold profiles differed across muscles. TA responses were predominantly below baseline at early ISIs and approached baseline at later intervals, with a small late positive peak. SOL showed an early increase above baseline that reached its maximum at approximately MEP + 40–50 ms and remained slightly above baseline across much of the later ISI range. GAS showed an early transition from below-baseline to above-baseline responses, followed by a return to below-baseline values at later ISIs. Despite these pooled tendencies, individual profiles frequently differed in peak location, response magnitude, and response direction, indicating that the population-level curves did not fully represent participant-specific ISI–response relationships. Participant-specific GP fits for the adult motor- and sensory-threshold conditions and children motor-threshold condition are provided in Supplementary Figures S7–S15.

3.4 GP model performance

At the participant-specific data-driven length scales, the GP reproduced the complete per-ISI response profiles in adults with a mean R^2 of 0.91 ± 0.11. It explained 0.55 ± 0.17 of the single-trial variance, compared with an empirical variance ceiling of 0.59 ± 0.14. Leave-one-ISI-out cross-validation, summarized at the participant-specific cross-validation-optimal length scales, resulted in a mean R^2 of 0.71 ± 0.20 (Fig. 4A, B). In children, the GP reproduced the complete per-ISI response profiles with a mean R^2 of 0.66 ± 0.38. It explained 0.35 ± 0.23 of the single-trial variance, compared with an empirical variance ceiling of 0.47 ± 0.16. Leave-one-ISI-out prediction resulted in a mean R^2 of 0.18 ± 0.28 (Fig. 4D, E). The pediatric results showed greater variability across participants.

3.5 Data efficiency

Using one repetition per ISI, GP regression recovered the reference response profiles more accurately than empirical per-ISI averaging in both groups (Fig. 4C, F). In adults, the one-repetition GP achieved a mean R^2 of 0.66 ± 0.19, compared with an R^2 of 0.19 ± 0.55 for empirical averaging. The performance of the one-repetition GP was approximately equivalent to empirical averaging with two repetitions per ISI; an advantage of empirical averaging over GP regression emerged only

from four complete repetitions per ISI, corresponding to 104 stimulations across the 26 tested ISIs. In children, the one-repetition GP achieved a mean R^2 of 0.20 ± 0.30, compared with an R^2 of -0.46 ± 1.42 for empirical averaging. In contrast to adults, empirical averaging became more accurate than GP regression from two repetitions per ISI onward. Corresponding GP model-performance and data-efficiency analyses for SOL and GAS under motor-threshold PNS are shown in Supplementary Figures S16 and S17, respectively.

3.6 Bayesian optimization

In adults, GPBO reached the 0.90 exploration-score threshold in 9 of 10 participants, the same number as random sampling. Among participants reaching the threshold, the median number of stimulations required was 10 [IQR: 8–17] for GPBO and 20 [IQR: 13–66] for random sampling. Across all participants, the final exploration score was 0.978 ± 0.015 for GPBO and 0.951 ± 0.022 for random sampling. The group exploration-score trajectories are shown in Fig. 5A.

In children, GPBO reached the 0.90 threshold in 5 of 8 participants, compared with 4 of 8 with random sampling. Among participants reaching the threshold, the median number of stimulations required was 45 [IQR: 24–60] for GPBO and 56 [IQR: 35–79] for random sampling. Across all participants, the final exploration score was 0.922 ± 0.025 for GPBO and 0.902 ± 0.023 for random sampling. The corresponding group exploration-score trajectories are shown in Fig. 5C.

3.7 Population-informed initialization

In adults, GPBO with the population-informed prior reached the 0.90 exploration-score threshold in 9 of 10 participants, the same number as GPBO without the prior. Among participants reaching the threshold, the median number of stimulations required was 7 [IQR: 6–20] with the population-informed prior and 10 [IQR: 8–17] without the prior. Across all participants, the final exploration score was 0.977 ± 0.016 with the prior and 0.978 ± 0.015 without the prior. The group exploration-score trajectories with and without the population prior are compared in Fig. 5B.

In children, GPBO with the population-informed prior reached the threshold in 6 of 8 participants, compared with 5 of 8 without the prior. Among participants reaching the threshold, the median number of stimulations required was 41 [IQR: 24–59] with the population-informed prior and 45 [IQR: 24–60] without the prior. Across all participants, the final exploration score was 0.929 ± 0.024 with the prior and 0.922 ± 0.025 without the prior. The corresponding group exploration-score trajectories are shown in Fig. 5D. Participant-specific threshold-crossing times and final exploration scores for GPBO, random sampling, and GPBO with population-informed initialization are summarized in Table 2. Corresponding Bayesian-optimization and population-informed initialization results for SOL and GAS are shown in Supplementary Figures S18 and S19, respectively.

Table 2
Participant-specific Bayesian-optimization performance with random sampling and population-informed initialization.

		Number of stimulations to reach 0.90			Final exploration score		
Group	Participant	GPBO	Random	GPBO + population prior	GPBO	Random	GPBO + population prior
Adults	P1	8	19	6	1	0.97	0.997
	P2	10	20	10	0.996	0.988	0.999
	P3	5	9	4	0.996	0.985	0.998
	P4	21	48	26	0.984	0.968	0.977
	P5	21	186	7	0.997	0.928	0.998
	P6	Not reached	Not reached	Not reached	0.851	0.765	0.84
	P7	8	8	6	0.997	0.998	0.999
	P8	16	119	44	0.964	0.941	0.967
	P9	9	14	6	0.993	0.982	0.995
	P10	14	26	18	1	0.988	0.996
Children	P1	19	39	24	0.978	0.97	0.982
	P2	56	85	49	0.953	0.943	0.961
	P3	Not reached	Not reached	Not reached	0.841	0.815	0.848
	P4	70	Not reached	59	0.968	0.868	0.979
	P5	Not reached	Not reached	Not reached	0.803	0.828	0.804
	P6	45	73	33	0.963	0.936	0.958
	P7	Not reached	Not reached	145	0.88	0.87	0.908
	P8	25	31	23	0.991	0.982	0.99

3.8 Protocol tolerability and MVC

Pain and fatigue ratings remained low. In adults, pain was 1.14 ± 0.82 for motor-threshold PNS and 0.63 ± 0.57 for sensory-threshold PNS, with median values of 1 [IQR: 1–2] and 1 [IQR: 0–1], respectively. The difference between PNS conditions was not significant, $p = 0.059$. Fatigue was 1.63 ± 1.10 for motor-threshold PNS and 1.45 ± 1.04 for sensory-threshold PNS, with median values of 1 [IQR: 1–2] and 1 [IQR: 1–2], respectively. The difference between PNS conditions was not significant, $p = 0.441$. Pain was not associated with ISI, $p = 0.145$, or test order, $p = 0.323$. Fatigue was not associated with ISI, $p = 0.366$, but slightly increased with test order, $\rho = 0.326$, $p < 0.001$. In children for motor-threshold PNS, pain was 1.79 ± 1.97, with a median value of 1 [IQR: 0–4]. Fatigue was 3.60 ± 1.72, with a median value of 4 [IQR: 2–5]. Pain was not associated with ISI, $p = 0.769$, but decreased with test order, $\rho = -0.20$, $p = 0.002$. Fatigue was not associated with ISI, $p = 0.827$, or test order, $p = 0.142$.

MVC changes did not differ significantly from zero in adults for TA motor, *p = 0.557*, TA sensory, *p = 0.232*, SOL motor, *p = 0.492*, SOL sensory, *p = 0.770*, GAS motor, *p = 0.275*, or GAS sensory, *p = 0.492*. In children, only motor-threshold PNS was considered, and MVC changes did not differ significantly from zero for TA, *p = 0.945* SOL, *p = 0.390*, or GAS, *p = 0.250.*

4. Discussion

This study combined dense, latency-referenced mapping of lower-limb PNS–TMS interactions with participant-specific Gaussian process modeling and retrospective Bayesian optimization. Conditioned MEP responses varied with ISI, PNS condition, muscle, and participant, with clearer timing-dependent modulation under motor-threshold than sensory-threshold PNS in adults. Participant-specific GPs represented adult motor-threshold TA profiles accurately and provided relatively strong prediction of responses at omitted ISIs, whereas pediatric model performance was lower and more variable. GP modeling also improved profile recovery when only one repetition per ISI was available, although this advantage was more sustained in adults. Finally, GPBO generally identified high-performing ISIs more efficiently than random sampling, particularly in adults, while population-informed initialization showed mixed and participant-dependent effects without a consistent reduction in stimulation requirements. Together, these findings support individualized modeling of lower-limb PNS–TMS timing but also show that model reliability and optimization efficiency cannot be assumed to be equivalent across participants or age groups.

4.1 Timing-, intensity-, and muscle-dependent responses

In adults, the pooled motor-threshold TA and SOL profiles were predominantly below the unconditioned baseline at earlier ISIs and increased toward or above baseline at later timings. GAS showed a less uniform response, with smaller above-baseline regions at both earlier and later ISIs. In contrast, sensory-threshold profiles remained relatively close to baseline across the tested timing range. These findings are consistent with upper-limb studies showing that peripheral afferent input can reduce or increase corticospinal responses depending on the timing and intensity of the conditioning stimulus [4, 5]. However, lower-limb timing windows should not be transferred directly from upper-limb protocols because of differences in conduction distance, spinal circuitry, corticospinal organization, muscle activation, and afferent processing [22].

The earlier below-baseline TA responses under motor-threshold PNS may reflect afferent inhibition-like interactions in which the peripheral volley reaches central sensorimotor pathways before TMS and transiently reduces the subsequent corticospinal response [23]. Their magnitude and duration may also depend on the fibers recruited by PNS. Motor-threshold stimulation likely generated a stronger and broader afferent volley than sensory-threshold stimulation, including greater recruitment of proprioceptive afferents, which is consistent with evidence that afferent inhibition depends on afferent-volley amplitude [24]. At later ISIs, the pooled adult TA profile increased above baseline, particularly around MEP + 95 to MEP + 115 ms, possibly reflecting a change in how the afferent input interacted with cortical and sensorimotor circuits after the earlier inhibitory influence had diminished. Nevertheless, these ranges represent descriptive group-level tendencies rather than statistically confirmed inhibition or facilitation at every individual ISI.

Responses also differed across muscles. TA showed the clearest transition from earlier below-baseline responses toward higher responses at later ISIs, which may partly reflect the experimental design: common peroneal nerve stimulation, the TA cortical hotspot, and active dorsiflexion were all selected primarily to target TA [17]. SOL showed a similar but less pronounced late increase, whereas GAS displayed a more variable profile. Because SOL and GAS were not directly targeted by the stimulation site or TA hotspot, their responses may have been influenced by differences in task-related activation, reciprocal inhibition, and muscle-specific corticospinal organization [25, 26]. Their profiles should therefore be interpreted as secondary muscle responses within a TA-optimized protocol rather than independently optimized timing functions.

4.2 Pediatric response profiles

Children showed significant ISI-dependent modulation in TA, SOL, and GAS under motor-threshold PNS, but their response profiles were more variable and differed from those of adults. Pediatric TA responses were predominantly below baseline at early ISIs and approached baseline later, with only a small late positive peak. SOL showed an earlier above-baseline maximum around MEP + 40 to MEP + 50 ms, whereas GAS transitioned from below baseline at early ISIs to above baseline at intermediate timings before returning below baseline later.

Lower-limb PNS–TMS conditioning has not been studied in children, and the present findings indicate that pediatric timing profiles should not be assumed to reproduce adult responses. Ongoing maturation of myelination, corticospinal organization, motor-cortex excitability, intracortical inhibition and facilitation, and sensorimotor integration may influence the timing and consistency of conditioned responses [27, 28]. Referencing ISIs to individual MEP latency accounted partly for corticospinal output timing but not for differences in peripheral afferent conduction or central afferent processing. The same latency-referenced ISI may therefore represent different physiological interactions across participants and age groups. However, the greater pediatric variability should not be attributed exclusively to neurodevelopment, because children also completed fewer repetitions per ISI, which may have contributed to noisier reference profiles and weaker model performance.

4.3 Participant-specific GP modeling

GP regression provided a continuous representation of the ISI–response relationship while accounting for correlations between neighboring timings and uncertainty in the estimated response function [9]. This was particularly relevant because the participant-specific curves differed substantially in magnitude, shape, and peak timing, and the pooled curves did not fully represent individual responses.

In adults, the strong agreement with the complete profiles and relatively good prediction of omitted ISIs indicated that the responses generally contained a reproducible temporal structure that could be modeled across neighboring timings. Prediction was poor at very short length scales but improved at moderate length scales, suggesting that adult response profiles generally contained a smooth structure that could be interpolated across neighboring ISIs. Very short length scales appeared more sensitive to local variation and noise, whereas moderate smoothing better balanced profile fit and prediction.

Pediatric GP performance was lower and more heterogeneous. Although the models could describe portions of the observed pediatric profiles, substantially weaker leave-one-ISI-out performance indicated that this fitted structure did not consistently generalize to entirely unobserved timings. The lower predictive performance may partly reflect the smaller amount of data available in children, who completed fewer repetitions per ISI and were assessed at only one PNS intensity. This distinction between fitting and generalization is important, because a model may reproduce the observations used for estimation while providing limited information about an omitted ISI.

4.4 Data efficiency

Beyond model fit and generalization, the GP framework was also evaluated for its ability to recover participant-specific response profiles from reduced datasets. GP regression was most advantageous under highly sparse sampling. With one repetition per ISI, the GP recovered the complete-repetition reference profile more accurately than independent empirical per-ISI averaging in both groups. In adults, the one-repetition GP approximately matched the performance of empirical averaging with two repetitions per ISI, indicating that information shared across neighboring ISIs could partially compensate for the absence of repeated measurements [29].

In children, the GP also outperformed empirical averaging with one repetition per ISI, but empirical averaging became more accurate from two repetitions onward. The present findings therefore do not support a general reduction in

pediatric repetition requirements. Rather, they illustrate the main advantage of GP regression in a low-repetition regime, where information shared across neighboring ISIs allows interpolation of the response profile when direct observations are sparse. As additional repetitions become available, empirical per-ISI estimates become increasingly reliable and the benefit of GP smoothing is expected to diminish [30]. The complete-repetition profile used for comparison should also be regarded as the best experimental reference available in this dataset, not as a true physiological ground truth. This likely provides a conservative estimate of the benefit of GP regression, because deviations of the smoothed GP estimate from residual noise in the complete-repetition reference profile are treated as prediction errors even when the GP may more closely approximate the underlying physiological response.

4.5 Bayesian optimization

The retrospective Bayesian-optimization analysis evaluated whether sequential single-trial sampling could identify a high-performing participant-specific ISI more efficiently than exhaustive mapping. GPBO uses the current GP posterior and its uncertainty to guide sequential sampling toward potentially high-performing ISIs [31].

In adults, GPBO reached high-performing ISIs more rapidly than random sampling while producing a similar overall threshold-reaching rate. Because the random condition used the same GP recommendation rule and differed only in how the next ISI was selected, this comparison isolates the benefit of GPBO-guided ISI selection rather than comparing GP modeling with a fully model-free procedure [32].

Optimization was less consistent in children, with a smaller advantage of GPBO over random sampling. The longer and more variable pediatric searches were consistent with the weaker leave-one-ISI-out GP prediction observed in this group. The smaller number of repetitions per ISI in the pediatric protocol may also have contributed to this lower predictive reliability by increasing uncertainty in the response estimates used to fit the surrogate model. When the surrogate model cannot reliably interpolate across unobserved timings, it provides less reliable guidance for sequential sampling. Thus, the poorer pediatric optimization performance may reflect not only limitations in model guidance but also the greater difficulty of defining a stable high-performing ISI when responses themselves are variable or poorly repeatable.

The exploration-score threshold represented identification of a high-performing ISI rather than necessarily the exact best observed 5-ms interval. This may be a more practical target than identifying the exact reference optimum when several neighboring ISIs produce similar responses. Nevertheless, flat, noisy, irregular, or narrowly peaked profiles reduced the advantage of guided sampling, and GPBO did not guarantee rapid convergence in every participant.

4.6 Population-informed initialization

Population-informed initialization did not provide a clear overall advantage. In adults, GPBO with and without the population-informed prior reached the threshold in 9 of 10 participants, with similar stimulation requirements and final exploration scores. In children, the prior allowed one additional participant to reach the threshold but did not consistently reduce stimulation requirements or improve final performance. Overall, the limited benefit of population-informed initialization suggests that participant-specific observations are more informative for optimization than response patterns derived from previous participants. This supports the need to identify high-performing ISIs individually for each new participant rather than assuming that population-level timing information will generalize reliably.

4.7 Pediatric tolerability and protocol burden

The protocol was well tolerated overall with no adverse events. Pain ratings were low in both groups, while fatigue was low in adults and moderate in children. One child discontinued because of impatience rather than a stimulation-related adverse effect. MVC did not decrease significantly, suggesting that perceived fatigue was not accompanied by a detectable reduction in voluntary force capacity. These findings are consistent with evidence supporting the safety and

tolerability of pediatric TMS [33] and controlled peripheral electrical stimulation in children [34]. Nevertheless, pediatric fatigue and the incomplete protocol emphasize the importance of reducing session duration and stimulation burden.

4.8 Clinical implications

The present findings may have important implications for lower-limb PAS protocols. The variation in conditioned MEP responses across ISIs suggests that stimulation timing influences whether PNS–TMS pairing produces a higher or lower acute response. However, because this study assessed immediate conditioned responses, the identified ISIs should be interpreted as candidate timing windows rather than confirmed plasticity-inducing parameters. The most effective timing may vary across individuals according to conduction times, sensorimotor organization, corticospinal excitability, clinical characteristics, fatigue, and rehabilitation goals. Therefore, a universal ISI may not be appropriate for all participants. A model-based framework could help select stimulation timings that better match each participant's physiological profile and could later be extended to personalize other parameters, including PNS intensity, TMS intensity, stimulation frequency, target muscle, and activation state. Prospective studies are required to determine whether ISIs associated with larger acute conditioned responses also produce stronger and more reliable long-term plasticity.

4.9 Limitations

This study should be interpreted considering its exploratory design. The sample was limited to 10 healthy adults and 8 typically developing children, restricting generalizability to clinical populations. The pediatric group also covered a relatively broad age range, and children completed fewer repetitions per ISI than adults, which may have contributed to their lower and more variable GP performance. The GP and Bayesian-optimization analyses were retrospective and based on replaying responses from a finite experimental dataset; therefore, their performance requires confirmation during prospective online optimization. In addition, the complete-repetition mean was used as the reference profile but remains an experimental estimate rather than a true physiological response function. Because unconditioned baseline MEPs were collected only once at the beginning of the protocol, temporal drift in corticospinal excitability cannot be excluded.

5. Conclusion

Taken together, this proof-of-concept study provides three main messages. First, lower-limb PNS–TMS conditioning was strongly timing dependent and was more pronounced under motor-threshold than sensory-threshold PNS in adults. Second, ISI–response profiles varied substantially across participants, muscles, and age groups, supporting participant-specific rather than universal timing selection. Third, GP modeling provided a continuous representation of participant-specific response profiles and improved profile recovery under highly sparse sampling, while GPBO identified high-performing ISIs more efficiently than random sampling, particularly in adults. Population-informed initialization did not provide a consistent advantage and showed strongly participant-dependent effects. These findings support further prospective evaluation of data-driven approaches for individualized lower-limb PNS–TMS timing.

Abbreviations

AMT
Active motor threshold
AUC
Area under the curve
BO
Bayesian optimization
CPN
Common peroneal nerve

EMG
Electromyography
GAS
Gastrocnemius medialis
GP
Gaussian process
GPBO
Gaussian process–based Bayesian optimization
GPML
Gaussian Processes for Machine Learning
IQR
Interquartile range
ISI
Interstimulus interval
MEP
Motor evoked potential
MSO
Maximum stimulator output
MVC
Maximal voluntary contraction
PNS
Peripheral nerve stimulation
RMS
Root mean square
RMT
Resting motor threshold
SD
Standard deviation
SEM
Standard error of the mean
SOL
Soleus
TA
Tibialis anterior
TMS
Transcranial magnetic stimulation

Declarations

Ethics approval and consent to participate

The study was approved by the Research Ethics Committee of Université de Montréal (protocol no. 2026-9243; approved 19 February 2026) and was conducted in accordance with the Declaration of Helsinki. All adult participants provided written informed consent prior to participation. For participants under 18 years of age, written informed consent was obtained from a parent or legal guardian, and verbal or written assent was obtained from the child when appropriate.

Consent for publication

Not applicable

Availability of data and materials

The data supporting the findings of this study are not publicly available because public data sharing is not permitted under the current ethics approval. Access to the data may be considered upon reasonable request to the corresponding author, subject to authorization by the Research Ethics Committee of Université de Montréal and compliance with applicable institutional and ethical requirements.

Competing interests

The authors declare that they have no competing interests

Funding

The first author was supported by the Natural Sciences and Engineering Research Council of Canada [CPRA - 610104 - 2026]. The last author holds a FRQS J1 Research Fellow salary grant. The project is also supported by funding the Courtois Foundation's Catalyst Program and from Interactive Technologies of Engineering in Rehabilitation Network (INTER).

The funders had no role in study design, data collection, analysis, interpretation, preparation of the manuscript, or the decision to submit the article for publication.

Author's contributions

MRE contributed to the conceptualization and design of the study, methodology development, data collection and curation, formal analysis, software development, validation, visualization, funding acquisition, resources, and preparation of the original manuscript. MT contributed to data collection and curation and methodology. MR contributed to the development and implementation of the GP and GPBO methodology, formal analysis, software development, and validation. MBe contributed to the conceptualization and design of the study, methodology, supervision, investigation, and validation. MBo contributed to the conceptualization and design of the study, development and implementation of the GP and GPBO methodology, formal analysis, software development, supervision, and validation. YC contributed to the conceptualization and design of the study, methodology, data collection and curation, funding acquisition, project administration, resources, supervision, validation, and visualization. MRE drafted the original manuscript. All authors critically reviewed and edited the manuscript and read and approved the final manuscript.

Acknowledgements

Not applicable

References

1. Coppola G, Di Lenola D, Abagnale C, Ferrandes F, Sebastianelli G, Casillo F, Di Lorenzo C, Serrao M, Evangelista M, Schoenen J, Pierelli F. Short-latency afferent inhibition and somato-sensory evoked potentials during the migraine cycle: surrogate markers of a cycling cholinergic thalamo-cortical drive?. The Journal of Headache and Pain. 2020;21(1):34.
2. Turco CV, El-Sayes J, Savoie MJ, Fassett HJ, Locke MB, Nelson AJ. Short-and long-latency afferent inhibition; uses, mechanisms and influencing factors. Brain stimulation. 2018;11(1):59-74.
3. Matur Z, Öge AE. Sensorimotor integration during motor learning: transcranial magnetic stimulation studies. Archives of Neuropsychiatry. 2017;54(4):358.

4. Motolese F, Todisco A, Celani LM, Musumeci G, Cruciani A, Norata D, Santoro F, Rossi M, Pilato F, Capone F, Di Lazzaro V. Short-latency afferent inhibition and modulation of contralateral and ipsilateral motor output: A neurophysiological study. Clinical Neurophysiology. 2025:2111397.
5. Fischer M, Orth M. Short-latency sensory afferent inhibition: conditioning stimulus intensity, recording site, and effects of 1 Hz repetitive TMS. Brain stimulation. 2011;4(4):202-9.
6. Roy FD, Gorassini MA. Peripheral sensory activation of cortical circuits in the leg motor cortex of man. The Journal of physiology. 2008;586(17):4091-105.
7. Roy FD, Yang JF, Gorassini MA. Afferent regulation of leg motor cortex excitability after incomplete spinal cord injury. Journal of neurophysiology. 2010;103(4):2222-33.
8. Kato T, Sasaki A, Nakazawa K. Short-and long-latency afferent inhibition of the human leg motor cortex by H-reflex subthreshold electrical stimulation at the popliteal fossa. Experimental Brain Research. 2023;241(1):249-61.
9. Seeger M. Gaussian processes for machine learning. International journal of neural systems. 2004 Apr;14(02):69-106.
10. Choinière L, Guay-Hottin R, Picard R, Lajoie G, Bonizzato M, Dancause N. Gaussian-process-based Bayesian optimization for neurostimulation interventions in rats. STAR protocols. 2024;5(1).
11. Garvey MA, Mall V. Transcranial magnetic stimulation in children. Clinical neurophysiology. 2008;119(5):973-84.
12. Teoli D, Dua A, An J. Transcutaneous electrical nerve stimulation. InStatPearls [Internet] 2024. StatPearls Publishing.
13. Hermens HJ, Freriks B, Disselhorst-Klug C, Rau G. Development of recommendations for SEMG sensors and sensor placement procedures. Journal of electromyography and Kinesiology. 2000;10(5):361-74.
14. Temesi J, Gruet M, Rupp T, Verges S, Millet GY. Resting and active motor thresholds versus stimulus–response curves to determine transcranial magnetic stimulation intensity in quadriceps femoris. Journal of neuroengineering and rehabilitation. 2014;11(1):40.
15. Mrachacz-Kersting N, Stevenson AJ. Paired associative stimulation targeting the tibialis anterior muscle using either mono or biphasic transcranial magnetic stimulation. Frontiers in human neuroscience. 2017;11:197.
16. Alder G, Signal N, Olsen S, Taylor D. A systematic review of paired associative stimulation (PAS) to modulate lower limb corticomotor excitability: implications for stimulation parameter selection and experimental design. Frontiers in neuroscience. 2019;13:895.
17. Knash ME, Kido A, Gorassini M, Chan KM, Stein RB. Electrical stimulation of the human common peroneal nerve elicits lasting facilitation of cortical motor-evoked potentials. Experimental brain research. 2003;153(3):366-77.
18. Roy FD, Norton JA, Gorassini MA. Role of sustained excitability of the leg motor cortex after transcranial magnetic stimulation in associative plasticity. Journal of Neurophysiology. 2007;98(2):657-67.
19. Jayaram G, Santos L, Stinear JW. Spike-timing-dependent plasticity induced in resting lower limb cortex persists during subsequent walking. Brain research. 2007;1153:92-7.
20. Nugent SM, Lovejoy TI, Shull S, Dobscha SK, Morasco BJ. Associations of pain numeric rating scale scores collected during usual care with research administered patient reported pain outcomes. Pain Medicine. 2021;22(10):2235-41.
21. Borg GA. Psychophysical bases of perceived exertion. Medicine & science in sports & exercise. 1982;14(5):377-81.
22. Carson RG, Kennedy NC. Modulation of human corticospinal excitability by paired associative stimulation. Frontiers in human neuroscience. 2013;7:823.
23. Tokimura H, Di Lazzaro V, Tokimura Y, Oliviero A, Profice P, Insola A, Mazzone P, Tonali P, Rothwell J. Short latency inhibition of human hand motor cortex by somatosensory input from the hand. The Journal of physiology. 2000;523(Pt 2):503.
24. Turco CV, El-Sayes J, Fassett HJ, Chen R, Nelson AJ. Modulation of long-latency afferent inhibition by the amplitude of sensory afferent volley. Journal of Neurophysiology. 2017;118(1):610-8.

25. Kesar TM, Stinear JW, Wolf SL. The use of transcranial magnetic stimulation to evaluate cortical excitability of lower limb musculature: challenges and opportunities. Restorative Neurology and Neuroscience. 2018;36(3):333-48.
26. Saito A, Nakagawa K, Masugi Y, Nakazawa K. Inter-muscle differences in modulation of motor evoked potentials and posterior root-muscle reflexes evoked from lower-limb muscles during agonist and antagonist muscle contractions. Experimental Brain Research. 2021;239(2):463-74.
27. Säisänen L, Julkunen P, Lakka T, Lindi V, Könönen M, Määttä S. Development of corticospinal motor excitability and cortical silent period from mid-childhood to adulthood–a navigated TMS study. Neurophysiologie Clinique. 2018;48(2):65-75.
28. Croarkin PE, Nakonezny PA, Lewis CP, Zaccariello MJ, Huxsahl JE, Husain MM, Kennard BD, Emslie GJ, Daskalakis ZJ. Developmental aspects of cortical excitability and inhibition in depressed and healthy youth: an exploratory study. Frontiers in human neuroscience. 2014;8:669.
29. Williams CK, Rasmussen CE. Gaussian processes for machine learning. Cambridge, MA: MIT press; 2006.
30. Ammann C, Guida P, Caballero-Insaurriaga J, Pineda-Pardo JA, Oliviero A, Foffani G. A framework to assess the impact of number of trials on the amplitude of motor evoked potentials. Scientific Reports. 2020;10(1):21422.
31. Shahriari B, Swersky K, Wang Z, Adams RP, De Freitas N. Taking the human out of the loop: A review of Bayesian optimization. Proceedings of the IEEE. 2015;104(1):148-75.
32. van Bueren NE, Reed TL, Nguyen V, Sheffield JG, van der Ven SH, Osborne MA, Kroesbergen EH, Cohen Kadosh R. Personalized brain stimulation for effective neurointervention across participants. PLoS computational biology. 2021;17(9):e1008886.
33. Allen CH, Kluger BM, Buard I. Safety of transcranial magnetic stimulation in children: a systematic review of the literature. Pediatric neurology. 2017;68:3-17.
34. Yan D, Vassar R. Neuromuscular electrical stimulation for motor recovery in pediatric neurological conditions: a scoping review. Developmental Medicine & Child Neurology. 2021;63(12):1394-401.

Figures

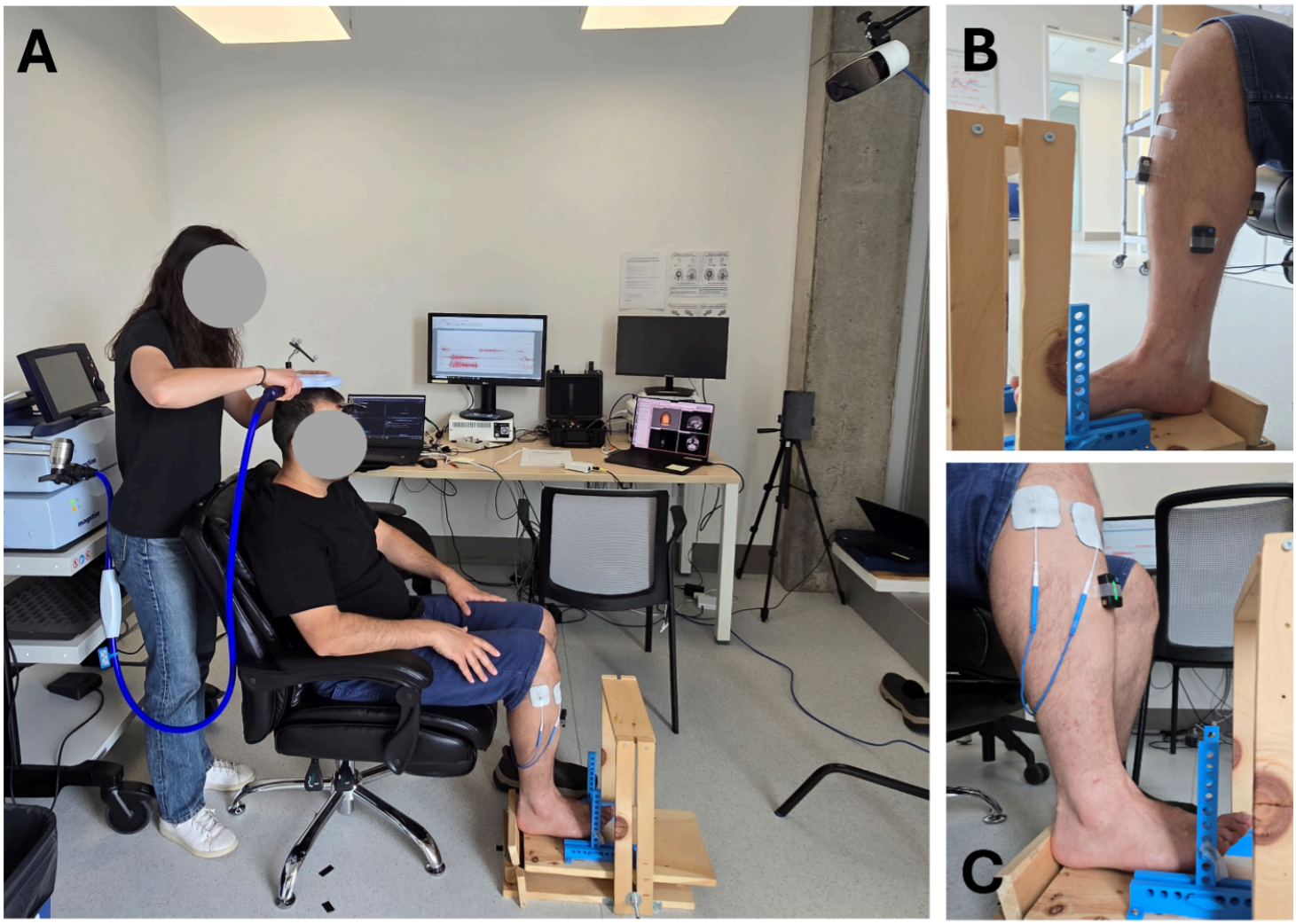


Figure 1

A. Experimental setup during the PNS-TMS sessions in an adult participant. B. Medial view of the targeted leg. C. Lateral view of the targeted leg.

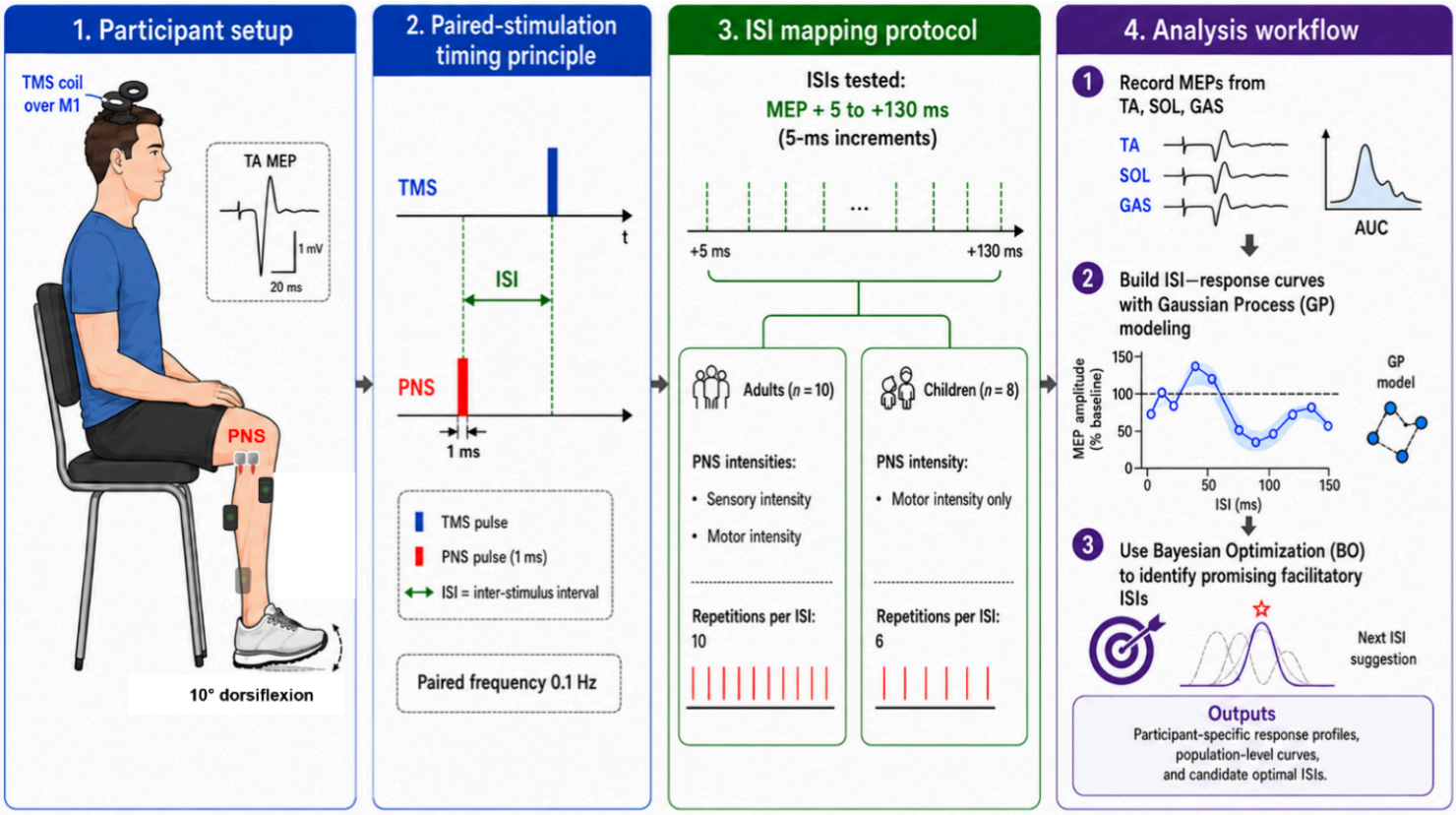


Figure 2

Schematic overview of the study procedure and analysis workflow. The figure illustrates the participant setup, the temporal relationship between PNS and TMS pulses, the individualized ISI mapping protocol, the repetition structure used in adults and children, and the subsequent analysis pipeline including AUC-based MEP quantification, Gaussian process modeling, and Bayesian optimization.

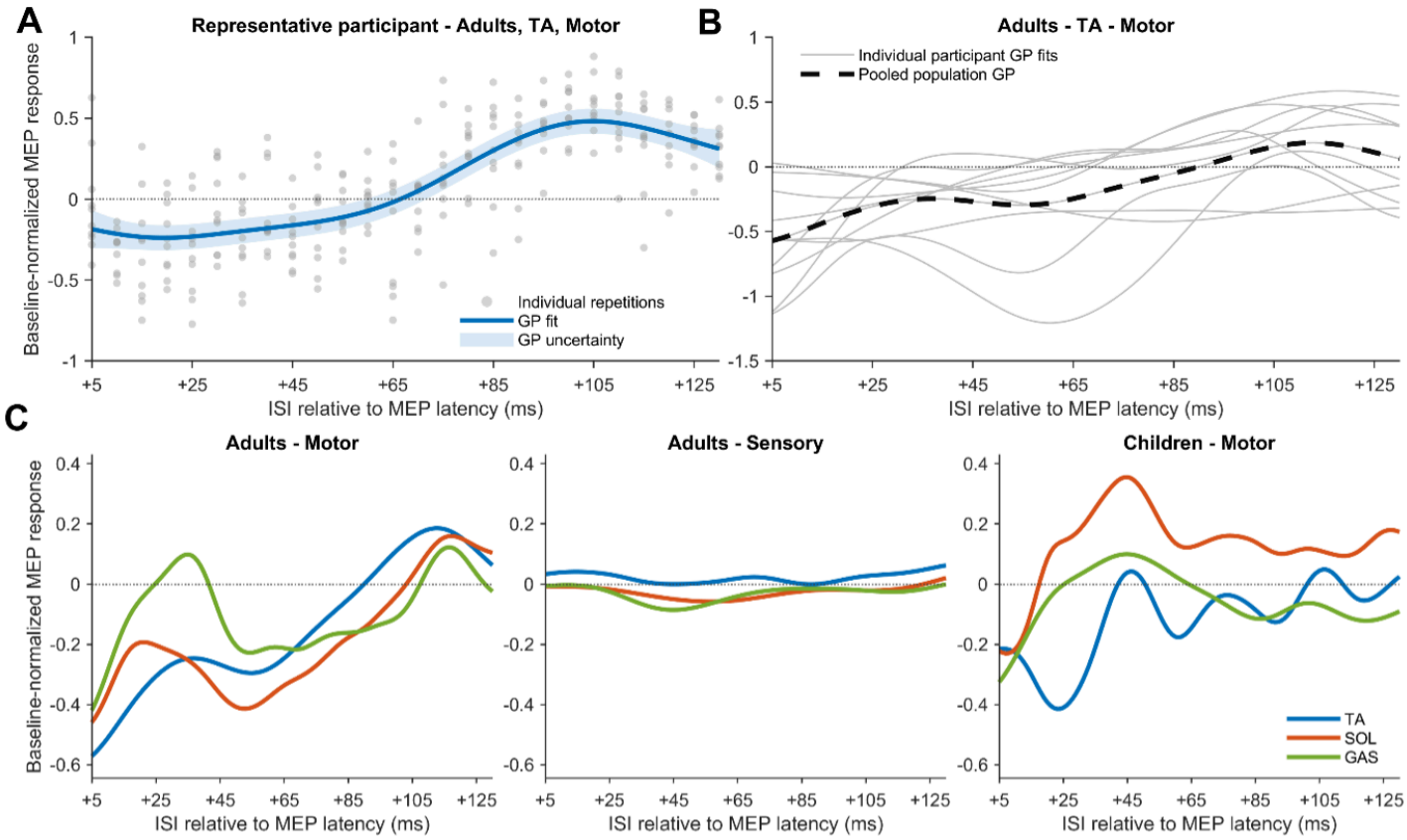


Figure 3

Participant-specific and pooled GP ISI–response profiles. (A) Representative participant-specific GP fit for the TA under the adult motor PNS condition, showing trial-level baseline-referenced MEP responses, the fitted GP, and its 95% credible interval. (B) Participant-specific GP fits for the adult TA motor PNS condition, with individual participant fits shown in gray and the pooled GP shown as a black dashed line. (C) Pooled GP ISI–response profiles for TA, SOL, and GAS under the adult motor, adult sensory, and children motor PNS conditions.

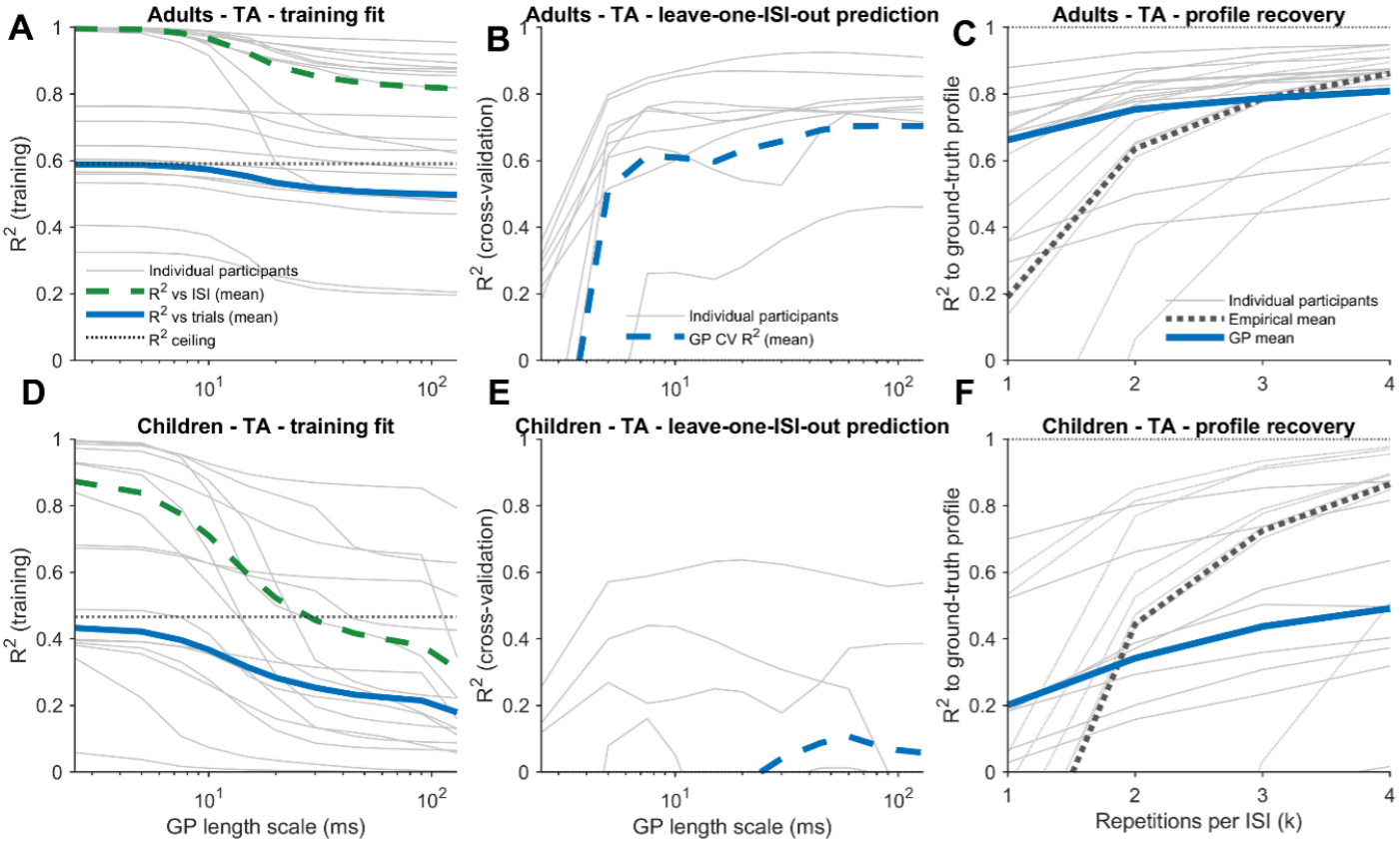


Figure 4

GP model performance and data efficiency for motor-threshold TA responses in adults and children. The top row shows adults and the bottom row shows children. (A,D) Training R^2 across GP length scales, showing model fit relative to the individual trial responses and complete per-ISI mean profiles, together with the empirical variance ceiling. (B,E) Leave-one-ISI-out cross-validation R^2 across GP length scales. The y-axis in these panels is restricted to 0–1 for visualization; negative R^2values are therefore outside the displayed range. (C,F) Recovery of the complete-repetition reference profile using GP regression and empirical per-ISI averaging across one to five repetitions per ISI. Thin gray lines represent individual participants, whereas thick lines represent group means.

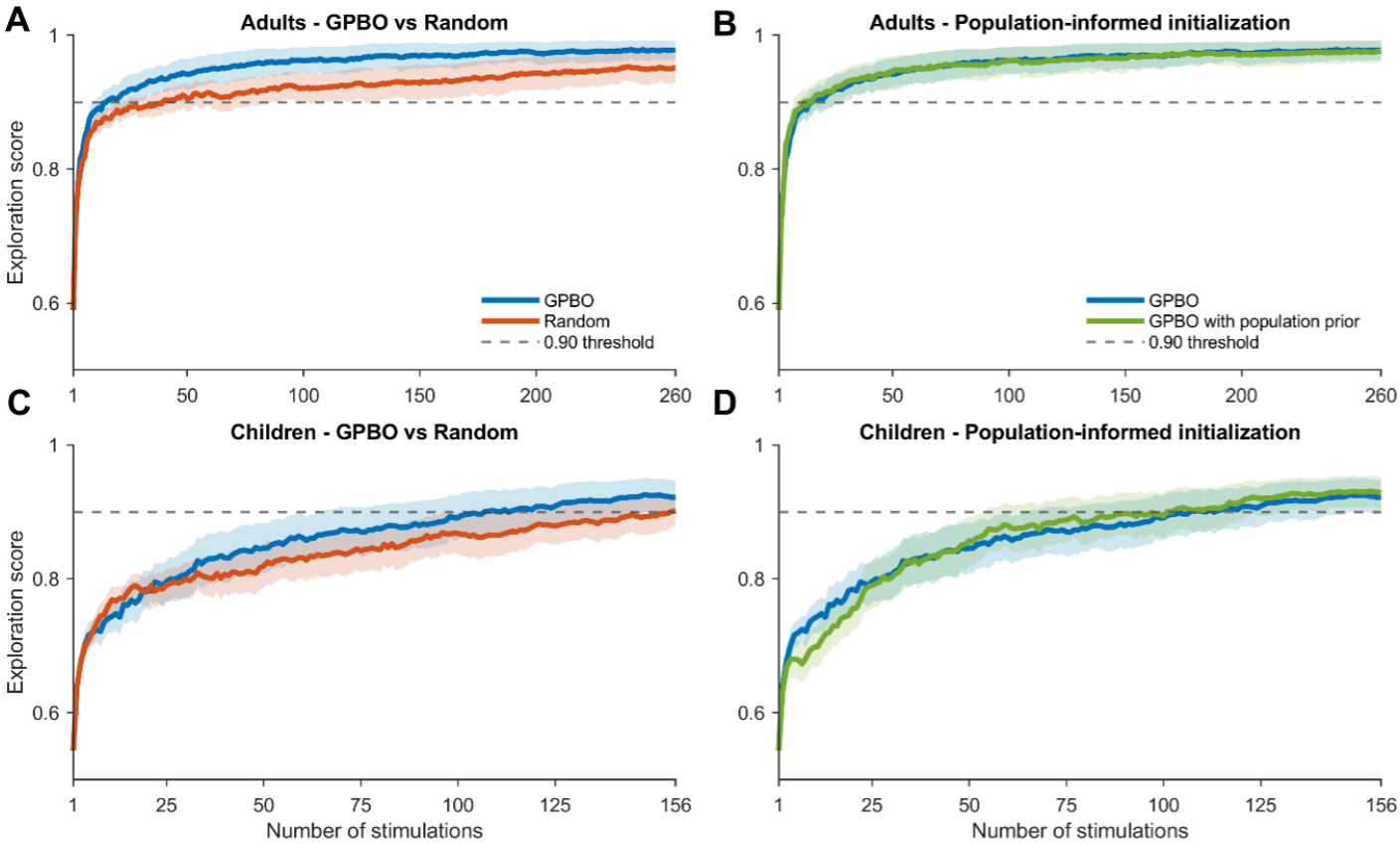


Figure 5

Bayesian-optimization performance and effect of population-informed initialization for motor-threshold TA responses in adults and children.(A, C) Exploration-score trajectories for GPBO and random sampling in adults and children, respectively. (B, D) Exploration-score trajectories for GPBO with and without a leave-one-participant-out population prior in adults and children, respectively. Solid lines represent group means, shaded regions represent the standard error of the mean across participants, and the horizontal dashed line indicates the exploration-score threshold of 0.90.

Supplementary Files

This is a list of supplementary files associated with this preprint. Click to download.

- Supplementarydocument.docx